Article

J. Biol. Regul. Homeost. Agents. 2024; 38(5): 3883–3897
https://doi.org/10.23812/j.biol.regul.homeost.agents.20243805.307

A Novel Gene Signature Based on Immunogenic Cell Death-Related Genes Predicts the Prognosis and Immune Infiltration Status of Melanoma Patients

Wei Li[1], Lin Li[1], Cheng Pang[1], Youqi Lu[1], Boyi Yang[2], Rumao Zhong[2], Yongzhen Liu[2], Lifeng Huang[2], Jinmin Zhao[3,*]

[1]Department of Bone and Joint Surgery, The First Affiliated Hospital of Guangxi Medical University, 530021 Nanning, Guangxi, China
[2]The First Clinical Medical College, Guangxi Medical University, 530021 Nanning, Guangxi, China
[3]Department of Trauma Orthopedic and Hand Surgery, The First Affiliated Hospital of Guangxi Medical University, 530021 Nanning, Guangxi, China
*Correspondence: drzhaojinmin@126.com (Jinmin Zhao)
Published: 1 May 2024

Background: The accumulating evidence suggests that immunogenic cell death (ICD) proves to be an effective therapeutic strategy for various tumors. This study aims to establish a model for the predictive evaluation of melanoma and investigate the potential clinical applications of ICD.
Methods: The mRNA profile data of melanoma samples, sourced from The Cancer Genome Atlas (TCGA) and Gene Expression Omnibus (GEO) databases, were employed to examine the expression patterns of genes associated with ICD in melanoma. Practical enhancement methods were applied to investigate the biological function of differentially expressed ICD-related genes. Multiple immune estimation approaches were employed to assess the infiltration of the immune landscape of samples in various clusters, aiming to explore the interaction between ICD and the immune system. Quantitative reverse transcription polymerase chain reaction (qRT-PCR) was used to validate the expression levels of key genes.
Results: Through unsupervised clustering analysis, melanoma patients were categorized into two distinct clusters based on the expression patterns of ICD-related genes. The overall survival rate was significantly higher in the group with elevated expression. The proportion of macrophages in the high-expression group was considerably greater. Additionally, ICD played a positive role in triggering anti-tumor immunity. Lastly, eight important candidate genes were identified to construct the prognostic model for melanoma patients. The qRT-PCR confirmed the increased level of BAX in melanoma cells, while decreased levels of ATG5, CASP8, CD8A, CXCR3, EIF2AK3, IFNG, and PIK3CA were observed.
Conclusions: This research illustrates the potential role of ICDs in the prognosis and treatment of melanoma. The development of a prognostic model based on this information could offer a reliable prognostic prediction for melanoma patients, aiding in the individualization of patient treatment.

Keywords: melanoma; immunogenic cell death; gene signature; immune infiltration; prognosis

Introduction

Melanoma, a malignant tumor arising from mutations in melanocytes triggered by ultraviolet radiation, familial lineage, and other factors [1], predominantly originates from the skin surface. However, there have been reports of primary melanoma occurring in the subcutaneous or sacral regions [2]. Despite the unknown exact pathogenesis, the incidence and mortality rates of malignant melanocytic tumors have been increasing globally in recent years. Malignant melanoma alone contributes to 72% of skin cancer deaths [3,4]. This is mainly due to the metastatic potential even in relatively small foci, leading to the difficulty of early diagnosis [5].

While surgical treatment can effectively cure most early-stage patients, chemotherapy is the chosen option for progressive cases, though it proves ineffective for the majority [6]. This underscores the importance of finding new treatment strategies. Several studies suggest that leveraging immunogenic cell death (ICD) could provide a novel approach to combatting cancer [7]. However, in recent years, there have been limited investigations into the potential clinical applications of ICD in melanoma immunotherapy [8]. Hence, it is crucial to explore the potential clinical utility of ICD in the context of melanoma immunotherapy and establish a predictive model for melanoma in a clinical setting.

The demise of neoplastic cells can be classified as immunogenic or nonimmunogenic, depending on the initiating stimulus [9]. Under a lethal external stimulus, neoplastic cells transition from a non-immune-stimulating state to an immunostimulatory state, triggering the immune system

Journal of
BIOLOGICAL REGULATORS
and Homeostatic Agents

to generate an anti-tumor response [9]. This process of immunogenicity transformation is known as ICD. Apart from CALR, which is exposed on the cell surface, several other molecules contribute to ICD, including HMGB1 released into the extracellular microenvironment by tumor cells, as well as particle aggregates and heat shock proteins (HSP) released by cells.

The ICD process also involves the generation of various signaling molecules termed damage-associated molecular patterns (DAMPs) [10]. DAMPs are particles that are secreted, released, or exposed on the surface of dying, stressed, or injured cells. These molecules serve as adjuvants or danger signals for the immune system. During ICD, DAMPs are produced and can bind to pattern recognition receptors (PRRs) on dendritic cells (DCs). This binding initiates a series of cellular chain processes that ultimately lead to the activation of both innate and adaptive immune defenses [10,11]. In the presence of damage-associated molecular patterns (DAMPs), tumor cells release numerous intracellular antigens, stimulating the immune system to recognize and eliminate them, effectively addressing the challenge of tumor immune evasion in immunotherapy [12].

In previous studies, ICD-related genes have demonstrated superior prognostic significance. Zhang *et al*. [13] conducted a study utilizing biological data from a public database on head and neck squamous cell carcinoma (HNSCC), revealing an association between immune cell dysfunction and alterations in the neoplasm microenvironment. Based on these findings, the researchers developed a predictive model specifically focused on ICD for HNSCC [13].

Xu *et al*. [14] found that tumor immunogenicity in triple-negative breast cancer (TNBC) patients was determined by the expression level of DAMPs and proposed a potential strategy associated with ICD for the treatment of TNBC. Furthermore, anti-neoplastic agents capable of inducing ICD are demonstrating promising applications in colon cancer prevention and therapy, as the exploration of ICD deepens [15].

Despite the ample data available on the subject, there is a lack of published research exploring the connection between the prognosis of melanoma and ICD-related genes. Therefore, based on extensive data from public databases, our study comprehensively investigated the mechanism and clinical utility of ICD in melanoma.

We utilized a publicly available dataset to examine 34 genes associated with ICD and conducted an analysis of their expression patterns, plausible mechanisms, and clinical implications in relation to melanoma. Additionally, we implemented a range of analyses to validate the prognostic signature by assessing the relevance between the risk score and clinical survival.

In summary, inducing an ICD-related prognostic signature could serve as a potential therapeutic modality for melanoma, given its significant inhibitory effect on melanoma cell growth. The model holds promise for early detection, as preventing early metastasis is crucial in treating melanoma. The ICD-related risk model presented herein, along with further mechanism studies, will contribute to achieving a valid clinical prognosis for melanoma patients.

Materials and Methods

Patients and Datasets

We incorporated groups of individuals diagnosed with melanoma from two databases, namely The Cancer Genome Atlas (TCGA, https://portal.gdc.cancer.gov/) and the Gene Expression Omnibus (GEO, https://www.ncbi.nlm.nih.gov/geo/). The training set consisted of 407 melanoma samples taken from the TCGA database, and the whole-transcriptional expression profiles of these melanoma samples were acquired. Correspondingly, the whole-transcriptional dataset GSE65904 from the GEO database, containing 214 melanoma samples, was used as the testing set. Both datasets from TCGA and GEO have a large-scale sample size with abundant clinical data, commonly utilized in previous studies. A total of 34 genes related to ICD were identified in earlier research and used in the present study [16].

Construction of the Network between ICD-related Proteins

To extract RNA-seq data for genes associated with ICD, we utilized the TCGA database. Employing the "limma" package, we successfully obtained differentially expressed genes (DEGs) related to ICD, filtering based on the criteria of $p < 0.05$ and |log2 fold change (FC)| >1. The identified DEGs were then subjected to the String database (https://string-db.org/) to retrieve interactions among the DEGs. Subsequently, the Cytoscape software (version 3.10.1) was employed to construct a protein-protein interaction (PPI) network that describes the interrelationships between these proteins.

Grouping ICD-related Genes Using Consensus Clustering

Through consensus cluster analysis, melanoma tumor samples were categorized into multiple subgroups. Utilizing the expression levels of ICD-related DEGs, optimal k-means clustering was performed, leading to the division of tumor samples into two clusters. Cluster 1 represents samples with highly expressed ICD-related DEGs, while Cluster 2 represents samples with low expressed ICD-related DEGs. The Principal Component Analysis (PCA) was conducted to validate the result of consensus cluster analysis.

A decision was made to assess the overall survival (OS) rate between the two clusters using the Kaplan-Meier (K-M) survival method.

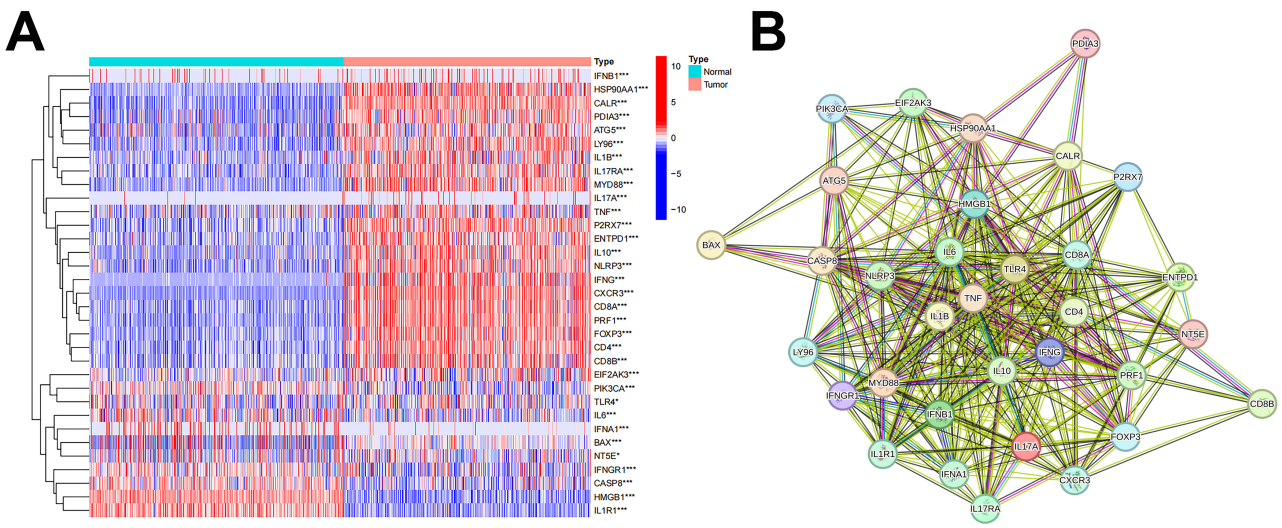

Fig. 1. Construction of the protein-protein interaction (PPI) network between immunogenic cell death (ICD)-related proteins. (A) The heatmap shows expression levels of 34 ICD-related genes in melanoma and normal samples based on the TCGA dataset. (B) The PPI network among 33 ICD-related DEGs. TCGA, The Cancer Genome Atlas; DEGs, differentially expressed genes.

Functional Analysis

All genes, whose expression levels reliably distinguish between Cluster 1 and Cluster 2 after being screened by threshold values of false discovery rate (FDR) <0.05 and $|\log2$ fold change (FC)$| > 1$, were selected as DEGs. Following the analysis of DEGs, we proceeded to conduct Gene Ontology (GO) and Kyoto Encyclopedia of Genes and Genomes (KEGG) analyses. These analyses were performed to determine the biological functions of DEGs and identify enriched pathways. Furthermore, Gene Set Enrichment Analysis (GSEA) was carried out based on ICD-related genes.

Comparison of Tumor-infiltrating Immune Cells among Different Clusters

Various methods were employed to assess immune infiltration patterns in different sample clusters, aiming to explore the relationship between ICD and the immune system. To determine the estimation, immune, and stromal scores for evaluating tumor purity between Cluster 1 and Cluster 2, the ESTIMATE method was utilized. The CIBERSORT algorithm (http://cibersort.stanford.edu/) was applied to assess the proportion of various immune cell types within melanoma tumor samples, encompassing a total of 22 distinct cell types. Differences in abundance between the two clusters were further examined.

To ascertain the connection between ICD and susceptibility to immunotherapy, immunological checkpoints and genes from the Human Leukocyte Antigen (HLA) family were successively evaluated.

Construction of an ICD-related Prognostic Signature

The "survival" package was employed to identify potential prognostic genes associated with OS in melanoma tumor patients, with a potential connection to ICD. Clinical survival data from TCGA, including OS and survival status, were collected along with ICD-related expression data for subsequent analysis. Using the Least Absolute Shrinkage and Selection Operator (LASSO) algorithm and 10-fold cross-validation, we determined the optimal penalty parameter (λ) based on the lowest deviation in partial likelihood. This process primarily screened the prognosis-related genes from 33 ICD-related DEGs.

To further identify major prognostic DEGs and obtain the corresponding linear regression model, the selected DEGs were sequentially subjected to univariate Cox regression and multivariate Cox regression using the R package "glmnet" (p-value < 0.05). The risk score for each patient was calculated using the following equation based on the linear regression model: Risk score = $\beta1 \times$ expG1 + $\beta2 \times$ expG2 + ... + βn $\times$ expGn, where β and expGn represent each core prognosis-related ICD DEGs regression coefficient and expression value, respectively.

Subsequently, a series of analyses were used to validate the prognostic signature's effectiveness. The Kaplan-Meier survival curve was utilized to compare the OS rate of patients across different groups. Additionally, we analyzed the expression profile, risk score distribution, and survival status in different groups.

Journal of
BIOLOGICAL REGULATORS
and Homeostatic Agents

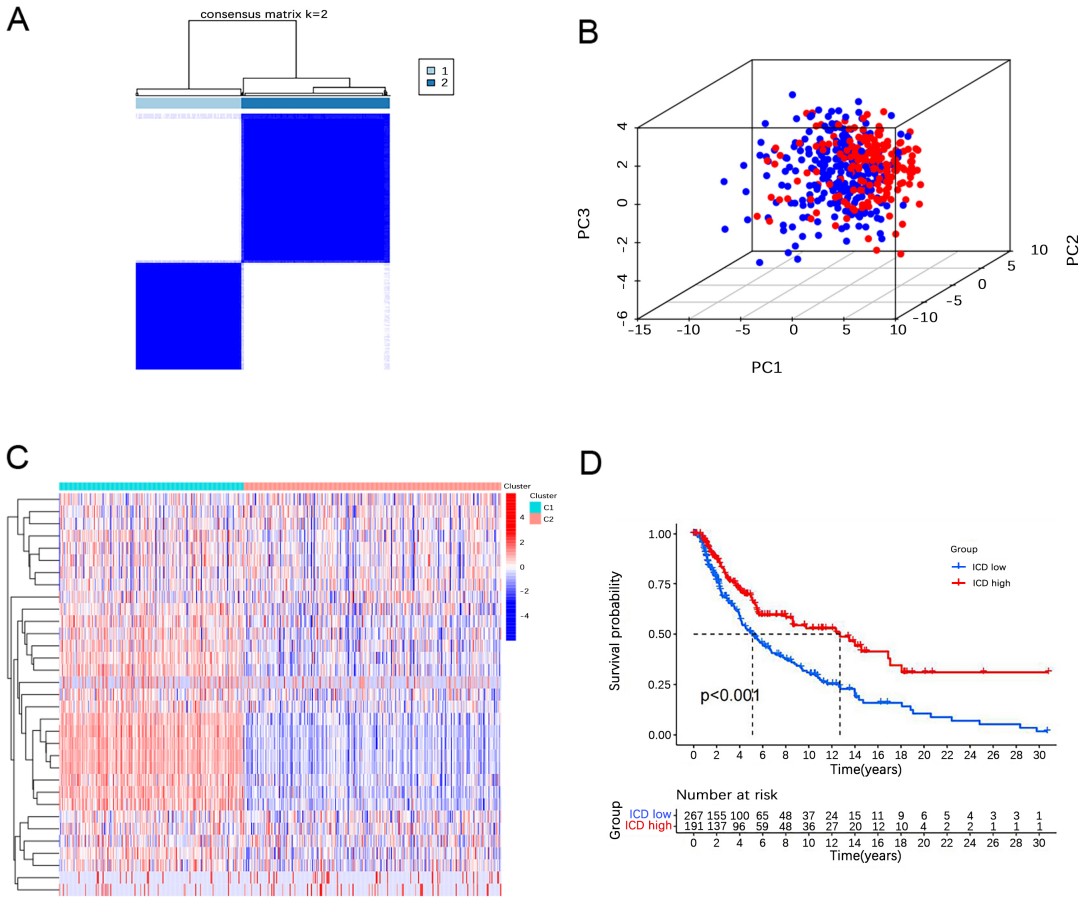

Fig. 2. Consensus clustering of ICD-related DEGs. (A) Patients were divided into 2 clusters based on consensus cluster analysis. (B) The PCA validated and visualized the distinctiveness of expressional pattern between Cluster 1 and Cluster 2. (C) The heatmap showed the expressional landscape of 33 ICD-related DEGs in 2 clusters. (D) The Kaplan-Meier curve suggests that patients in Cluster 1 have significantly higher overall survival rates (p-value < 0.001). PCA, Principal Component Analysis.

Validation of the Prognostic Signature

To ensure the accuracy of the predictive characteristics, we verified that the risk score equations used to compute the risk score of each patient were consistent with those employed in the training dataset.

Independent Prognostic Analysis

A univariate Cox analysis was conducted to assess the predictive value of each clinical parameter and the risk model. Subsequently, a multivariate Cox analysis for OS was employed to establish independent risk factors and determine whether the prognostic signature associated with ICD served as a predictor independent of other clinicopathological parameters.

Analyzing the Correlation between Risk Score and Immune Cells

The "limma" package was used to further explore the relationship between the proportion of specific immune cells and the risk scores of individual patients, with typical samples being disregarded.

Analysis of Quantitative Reverse Transcription Polymerase Chain Reaction (qRT-PCR)

HFF-1 cells (catalog number: CL-0352), representing normal human skin cells, and A-375 cells (catalog number: CL-0014), representing human melanoma cells, were obtained from Procell, a cell bank based in China. The provider of HFF-1 cells and A-375 cells conducted Short Tandem Repeats (STR) certification and mycoplasma testing. The cell culture medium used was a DMEM mixture supplemented with 10% fetal bovine serum. Once the cell confluence rate reached 70% to 80%, they were cultured in an incubator with a temperature of 37 °C, humidity at sat-

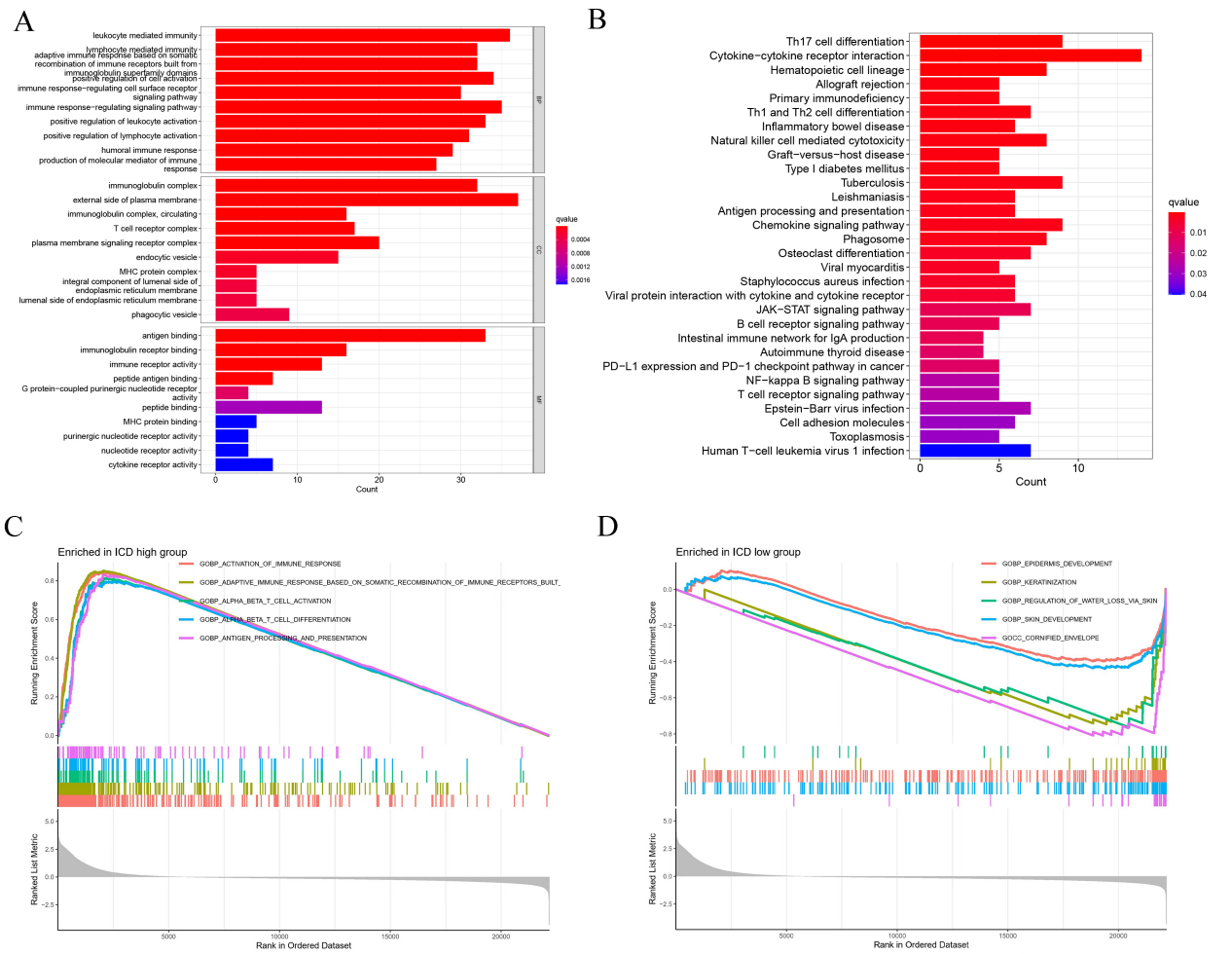

Fig. 3. Gene Ontology (GO), Kyoto Encyclopedia of Genes and Genomes (KEGG), and Gene Set Enrichment Analysis (GSEA). (A) The enrichment analysis based on GO analysis is comprised of biological process, cellular component, and molecular function. (B) The enrichment analysis based on KEGG. (C) The GSEA analysis of ICD-related genes in the high ICD score group. (D) The GSEA analysis of ICD-related genes in the low ICD score group.

uration, and 5% CO_2. Subsequently, the cells were treated with trypsin solution for digestion and subcultures. Cells in the logarithmic growth phase were selected for further investigation.

The RNA from each group was isolated using the TRIzol kit reagent (15596026, Invitrogen, Carlsbad, CA, USA) and subsequently converted into cDNA through reverse transcription utilizing the QuantiTect Reverse Transcription Kit (205311, QIAGEN, Hilden, Germany). Polymerase chain reaction (PCR) was performed using a real-time fluorescent signal to measure the amount of DNA in each PCR cycle. For PCR analysis, SYBR-Green (S7563, Invitrogen, Carlsbad, CA, USA) was used as a quantification tool. The PCR amplification consisted of 40 cycles, involving denaturation at 95 °C for 15 s, annealing at 60 °C for 30 s, and elongation at 60 °C for 30 s. The expression levels were then normalized relative to the GAPDH levels. Primer sequences are listed in Table 1. Data analysis adopted the $2^{-\Delta\Delta Ct}$ method.

Statistics

We employed Strawberry Perl for Windows (version 5.18.2) to process and organize the downloaded data. R version 3.6.1 was utilized for all data analysis. A significance level of $p < 0.05$ was considered statistically significant unless otherwise specified.

Journal of
BIOLOGICAL REGULATORS
and Homeostatic Agents

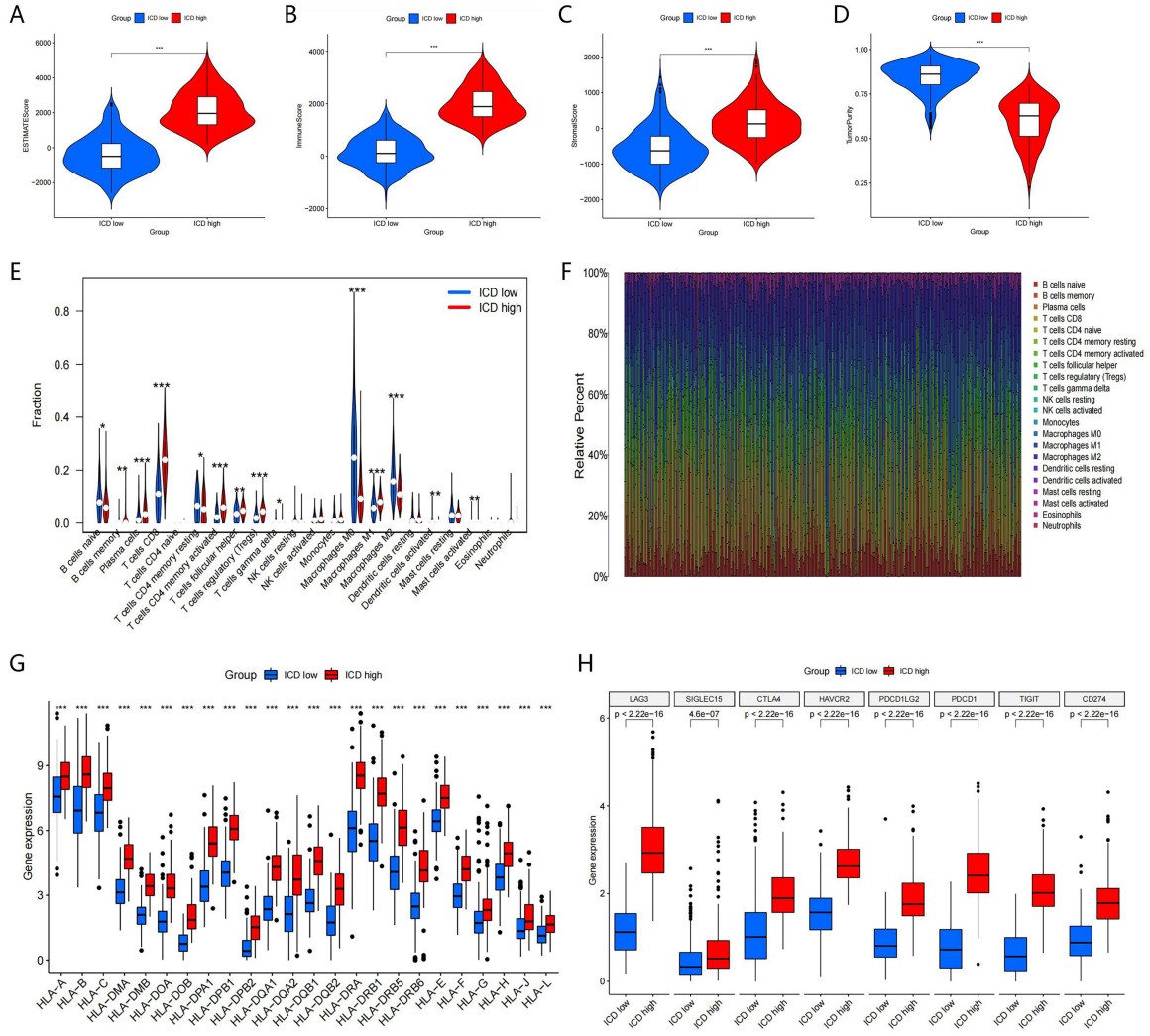

Fig. 4. Immune infiltration landscape analysis of melanoma patients in two clusters. (A) ESTIMATE score. (B) Immune score. (C) Stromal score. (D) Tumor purity. (E) The fraction of 22 types of immune cells in two clusters. (F) Histogram displaying the expression rate of the immune cells in 470 samples. (G) Comparison of the mRNA expression of human leukocyte antigen genes between two clusters. (H) Comparison of the mRNA expression of immune checkpoints between two clusters. The statistical significance was visualized by * in figure (p-value < 0.001: ***, p-value < 0.01: **, p-value < 0.05: *).

Results

Construction of the PPI Network between ICD-related Proteins

The differential analysis of RNA-seq data was conducted on TCGA melanoma samples to investigate the expression patterns of ICD-related genes. Among the 34 ICD-related genes, 33 genes exhibited differential expression in the melanoma samples. Notably, 23 of these genes were found to be upregulated, while 10 genes were downregulated. A heatmap was generated to visually represent the DEGs (Fig. 1A). Furthermore, the PPI network revealed a total of 618 interaction relationships among the 33 ICD-related DEGs (Fig. 1B).

Consensus Clustering of ICD-related Genes in Two Clusters with Different Prognosis

Through consensus cluster analysis, melanoma tumor samples were categorized into two clusters (K = 2), corresponding to highly expressed ICD-related genes and low-expressed ICD-related genes, based on the expression levels of 33 ICD-related DEGs (Fig. 2A). Patients with highly expressed ICD-related genes were assigned to Cluster 1, while others with low expressed ICD-related genes were classified into Cluster 2. Subsequent PCA demonstrated that the consensus cluster analysis effectively distinguished Cluster 1 and Cluster 2, indicating significant differences in expression patterns between the two clusters (Fig. 2B). The expression levels of ICD-related DEGs were illustrated in a heatmap (Fig. 2C), revealing that Cluster 1 exhibited higher

Table 1. Forward and reverse sequences of primers.

Primer	Forward Sequence (5′ to 3′)	Reverse Sequence (5′ to 3′)
GAPDH	AATCAAGTGGGGCGATGCTG	GCAAATGAGCCCCAGCCTTC
BAX	CGAACTGGACAGTAACATGGAG	CAGTTTGCTGGCAAAGTAGAAA
ATG5	GGACAGTTGCACACACTAGGAGATC	CTCAGATGTTCACTCAGCCACTGC
CASP8	TGCCTACAGGGTCATGCTCTATCAG	CCAGCAGGTTCATGTCATCATCCAG
CD8A	GGTCCTTCTCCTGTCACTGGTTATC	CCGAAAGGCTGGGCTTGTCTC
CXCR3	GCGGATGTGGATGCTGCTCTTG	AGACGATGGCTGCCTCTGGAG
EIF2AK3	ATGGATGATGTGGTCAAGGTTGGAG	TGTCTGGCATAAGCTGGCATTGG
IFNG	GAGTGTGGAGACCATCAAGGAAGAC	GCGTTGGACATTCAAGTCAGTTACC
PIK3CA	TTAGTTGAGCAAATGAGGCGACCAG	GCAGGGTTTAGAGGAGACAGAAAGC

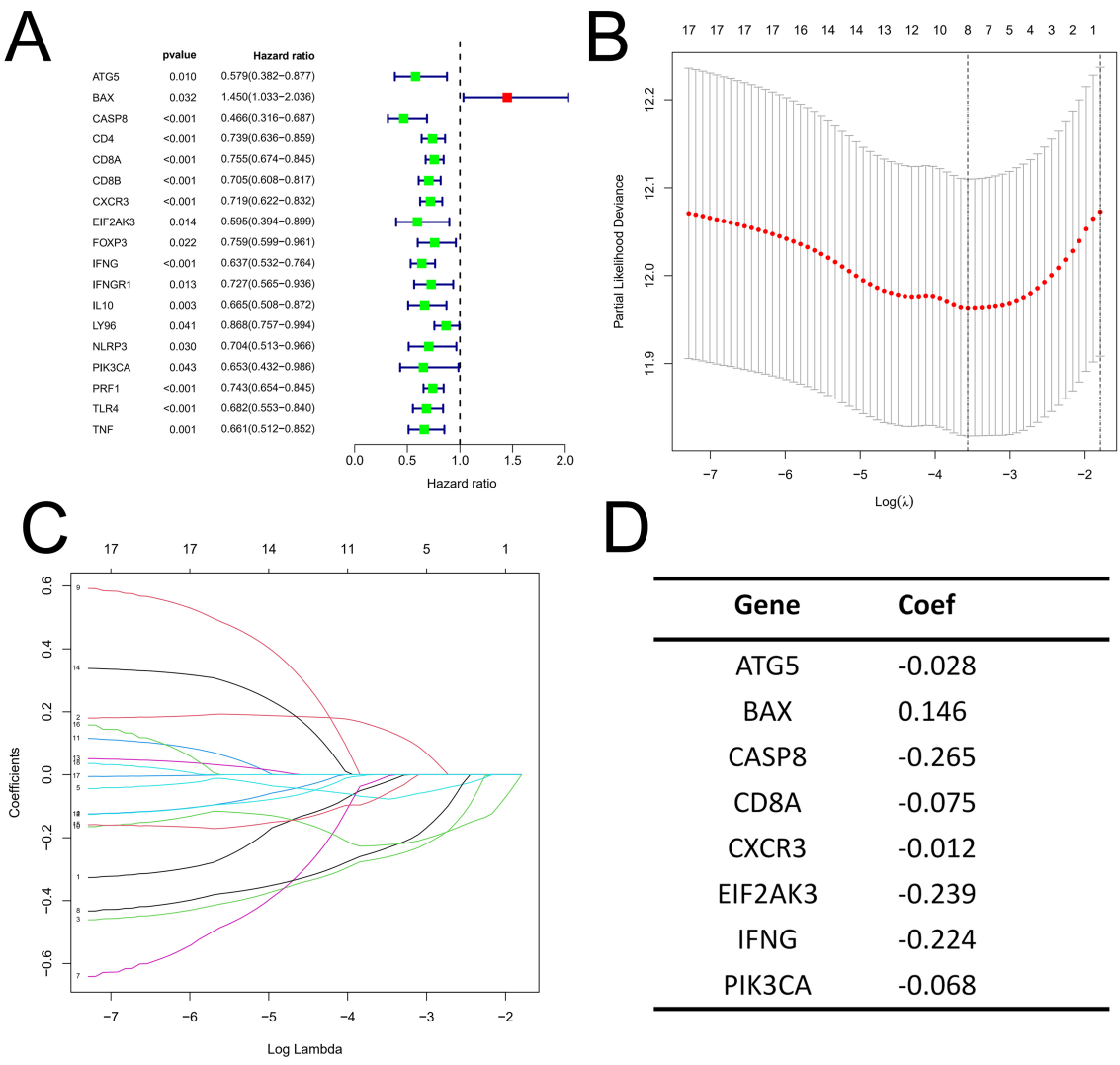

Fig. 5. Construction of the ICD-related prognostic signature based on the TCGA dataset. (A) The forest plot of 33 ICD-related DEGs relate to the overall survival (OS) rate of melanoma patients. (B) The optimal value of penalty lambda (λ) is selected in the Least Absolute Shrinkage and Selection Operator (LASSO) analysis. (C) LASSO coefficient profiles of 8 ICD-related DEGs. (D) The symbol names of 8 ICD-related DEGs and corresponding coefficients.

expression levels of ICD-related genes. According to the K-M survival analysis, Cluster 1 showed a higher OS rate (Fig. 2D).

Functional Enrichment Analysis

To identify genes exhibiting differential expression between Cluster 1 and Cluster 2, we employed the approach

Journal of
BIOLOGICAL REGULATORS
and Homeostatic Agents

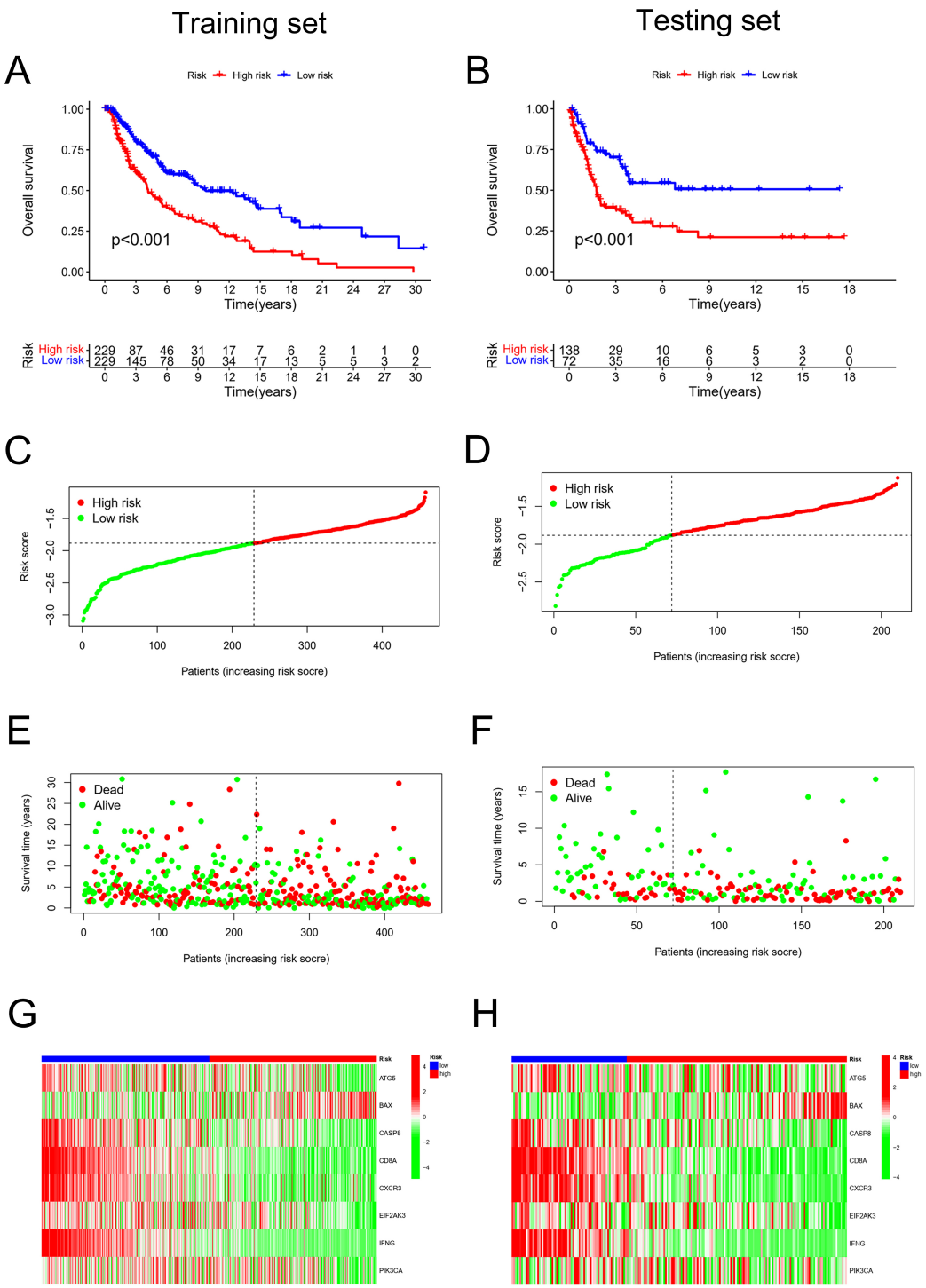

Fig. 6. Analysis and validation of ICD-related prognostic model in melanoma patients. (A) Kaplan-Meier (K-M) survival curves analysis of risk score in the training set. (B) K-M survival curves analysis of risk score in the testing set. (C) Distribution of risk score of melanoma patients in the training set. (D) Distribution of risk score of melanoma patients in the testing set. (E) Survival status of each patient in the training set. (F) Survival status of each patient in the testing set. (G) Heatmap showing the expression of ICD-related prognostic genes in the training set. (H) Heatmap showing the expression of ICD-related prognostic genes in the test cohort.

Table 2. Top 5 significant GO terms enriched in different ICD score groups, $p < 0.05$.

Group	GO terms	ES	NES	*p*-value
High	Activation of immune response	0.841	2.754	0.00
	Adaptive immune response based on somatic recombination of immune receptors built from immunoglobulin superfamily domains	0.852	2.787	0.00
	Alpha-beta T cell activation	0.813	2.552	0.00
	Alpha-beta T cell differentiation	0.796	2.437	0.00
	Antigen processing and presentation	0.832	2.544	0.00
Low	Epidermis development	–0.398	–1.893	0.00
	Keratinization	–0.747	–3.393	0.00
	Regulation of water loss via skin	–0.763	–2.313	0.00
	Skin development	–0.440	–2.012	0.00
	Cornified envelope	–0.809	–2.589	0.00

GO, Gene Ontology; ES, enrichment score; NES, normalized enrichment score.

detailed in the methods section and obtained the DEGs. GO and KEGG analyses were employed to elucidate the biological processes underlying the 33 ICD-related DEGs. Additionally, all 34 ICD-related genes were subjected to GSEA to further analyze functional enrichment.

The findings suggest that DEGs are notably linked to biological processes (BP) related to immune response mediated by leukocytes and the positive regulation of cell activation through the immunoglobulin superfamily domains. The DEGs were associated with various molecular functions, including antigen binding, binding to immunoglobulin receptors, and immune receptor activity, indicating a potential role in immune system function and response. In terms of Cellular Component (CC), DEGs were primarily enriched in the outer region of the plasma membrane, complexes involved in signaling on the plasma membrane, and complexes containing immunoglobulins (Fig. 3A).

The identified common DEGs in the MF item were predominantly associated with various biological processes, including Cytokine-cytokine receptor interaction, Tuberculosis, Th17 cell differentiation, and Chemokine signaling pathway, as revealed through KEGG pathway enrichment analysis (Fig. 3B).

To elucidate the differences in potential signaling pathways between the two clusters, the characterized GO pathways in different clusters were obtained through GSEA. The analysis of Fig. 3C,D revealed that the group with high ICD scores exhibited enrichment in alpha-beta T cell activation, alpha-beta T cell differentiation, antigen processing, and presentation. In contrast, the group with low ICD scores showed enrichment in epidermis development, keratinization, regulation of water loss through the skin, skin development, and cornified envelope.

The annotation analysis of these genes suggests that the expression patterns of ICD-related genes in melanoma are associated with immune disorder. Table 2 provides specific parameters of the significantly enriched GO terms.

Difference between Tumor-infiltrating Immune Cells and Immune Status between Different Clusters

Based on the ESTIMATE methodology, the ESTIMATE, immune, and matrix scores of Group 1 samples significantly exceeded those of Group 2 samples. Additionally, compared to Cluster 1, Cluster 2 demonstrated higher tumor purity (Fig. 4A–D). Two-cluster immune cell counts and displays were performed. According to the findings, Cluster 1 exhibited a higher proportion of plasma cells, CD8+ T cells, activated memory CD4+ T cells, follicular helper T cells, T regulatory cells (Tregs), and M1 macrophages compared to Cluster 2.

On the other hand, Cluster 2 is characterized by a greater proportion of mast cells in an active state, dendritic cells, naive B cells, memory B cells, memory resting CD4+ T cells, gamma delta T cells, M0 macrophages, and M2 macrophages (Fig. 4E,F).

A boxplot was created to display and compare the levels of Human Leukocyte Antigens (HLAs) between the two clusters. As shown in Fig. 4G, all HLA-related genes listed in the figure were expressed higher in Cluster 1. Specifically, Cluster 1 exhibited higher expression of mRNA for common immune checkpoints, including *LAG3*, *SIGLEC15*, *CTLA4*, *HAVCR2*, *PDCD1LG2*, *PDCD1*, *TIGIT*, and *CD274* (Fig. 4H).

Construction of the ICD-related Prognostic Signature in Melanoma

The information from the TCGA database was utilized to create the prognostic signature as a training set, while the GSE65904 dataset was employed to confirm the model's accuracy. A total of 470 patients were included in the model generation process due to their integrated and important clinical parameters. Among the 33 ICD-related DEGs, 18 exhibited a significant correlation with the OS of patients with melanoma tumors, as visually represented in a forest plot (Fig. 5A). After LASSO-Cox regression analysis, eight of the 18 prognostic ICD-related DEGs were identified as the best candidates for creating a prognostic sig-

Journal of
BIOLOGICAL REGULATORS
and Homeostatic Agents

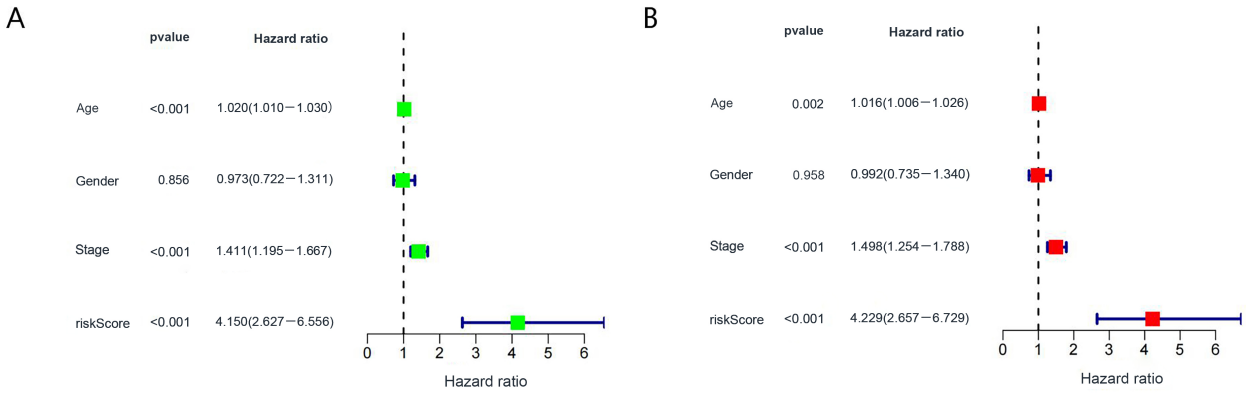

Fig. 7. Forest plot of Cox regression analysis. (A) Univariate Cox regression analysis showed the correlation between the OS rate and clinical characteristics. (B) Multivariate Cox regression analysis showed that the prognostic signature of ICD-related genes was an independent prognostic indicator for the OS of melanoma patients.

nature with the most potent prognostic value (Fig. 5B–D). Among these genes, *BAX* was designated as a risk gene, whereas *ATG5*, *CASP8*, *CD8A*, *CXCR3*, *EIF2AK3*, *IFNG*, and *PIK3CA* were considered protective genes.

Subsequently, an individualized risk score was calculated using the formula: Risk Score = (–0.028 × ATG5) + (0.146 × BAX) + (–0.265 × CASP8) + (–0.075 × CD8A) + (–0.012 × CXCR3) + (–0.239 × EIF2AK3) + (–0.224 × IFNG) + (–0.068 × PIK3CA). These risk scores were assigned to each melanoma patient. The results showed that high-risk melanoma patients had significantly worse OS (Fig. 6A). Cumulative distribution curve inflection points based on risk scores were used to divide melanoma patients into two cohorts of high and low-risk groups (Fig. 6C). Fig. 6E depicts the trend of patient survival status with increasing risk scores, where red dots represent deceased patients and green dots represent patients who are still alive. It appeared that low-risk patients had a higher survival rate.

The expression profile heatmap (Fig. 6G) indicated a significant increase in the expression of *BAX* in melanoma samples, while the expressions of *ATG5*, *CASP8*, *CD8A*, *CXCR3*, *EIF2AK3*, *IFNG*, and *PIK3CA* were significantly decreased.

Validation of the Prognostic Signature in Melanoma

The formulas used to generate risk scores in the training set were also applied to evaluate the predictive ability and consistency of the ICD-related DEGs-based prognostic models. The K-M survival curve indicated that the group with a lower risk exhibited a significantly better prognosis (Fig. 6B). Similar outcomes to the training set were observed in the distribution of risk scores (Fig. 6D), survival status (Fig. 6F), and expression profile heatmap (Fig. 6H).

In summary, these results suggested that the gene signature provided a reliable prediction of OS and held significant prognostic significance for individuals diagnosed with melanoma.

Independence Testing of the Constructed Prognostic Signature

The age, gender, and stage of melanoma tumor patients were then retrieved as critical clinical variables. Univariate and multivariate Cox regression analyses between these variables and risk scores derived from the prognostic signature were conducted to ascertain if ICD-related prognostic signatures are independent prognostic variables in melanoma patients. In addition to gender, univariate analyses showed strong associations between other clinical characteristics such as age, staging, prognostic features, and time to surgery (Fig. 7A). After additional confounding variables were eliminated, the risk score was identified as an independent predictive determinant of OS in melanoma patients (Fig. 7B).

Correlation Analysis of Risk Score and the Abundance of Immune Cells

The composition of specific immune cells in relation to risk scores is depicted in Fig. 8A–L There is an increase in the abundance of naive B cells, activated dendritic cells, M0 and M2 macrophages, and resting mast cells. The percentages of memory B cells, M1 macrophages, plasma cells, memory-activated CD4+ T cells, CD8+ T cells, follicular helper T cells, and Tregs decreased significantly with increasing risk scores, whereas the percentages of the other cell types did not show this correlation. These findings highlight the various immune infiltration patterns across melanoma patients in different risk groupings, suggesting a new avenue for further investigation into the underlying causes of ICD in melanoma patients.

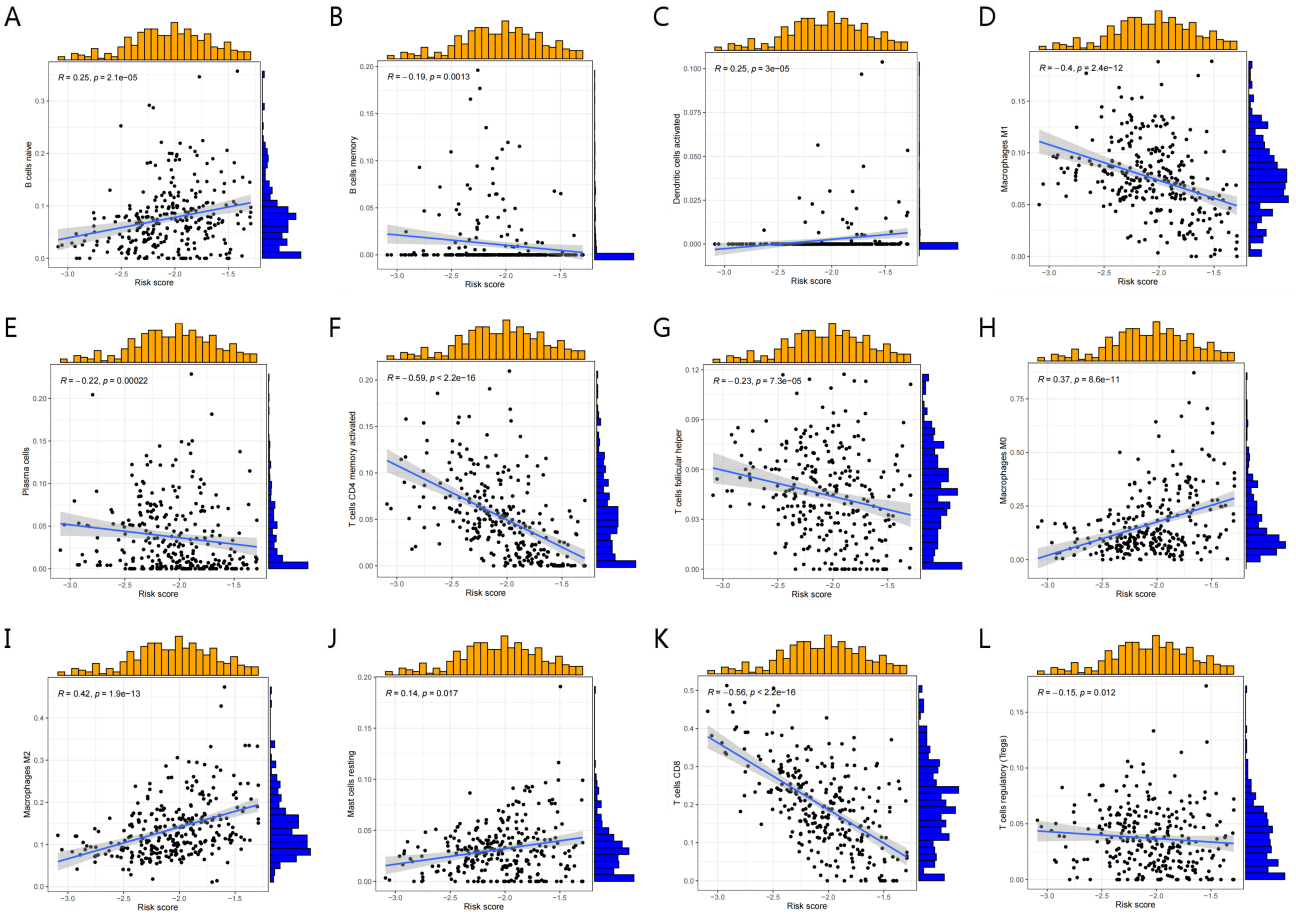

Fig. 8. Correlation analysis of risk score and the abundance of immune cells. The correlation between risk score and abundance of immune cells was shown by scatter plot. The yellow histogram (risk score) and blue histogram (immune cells abundance) exhibited the data distribution.

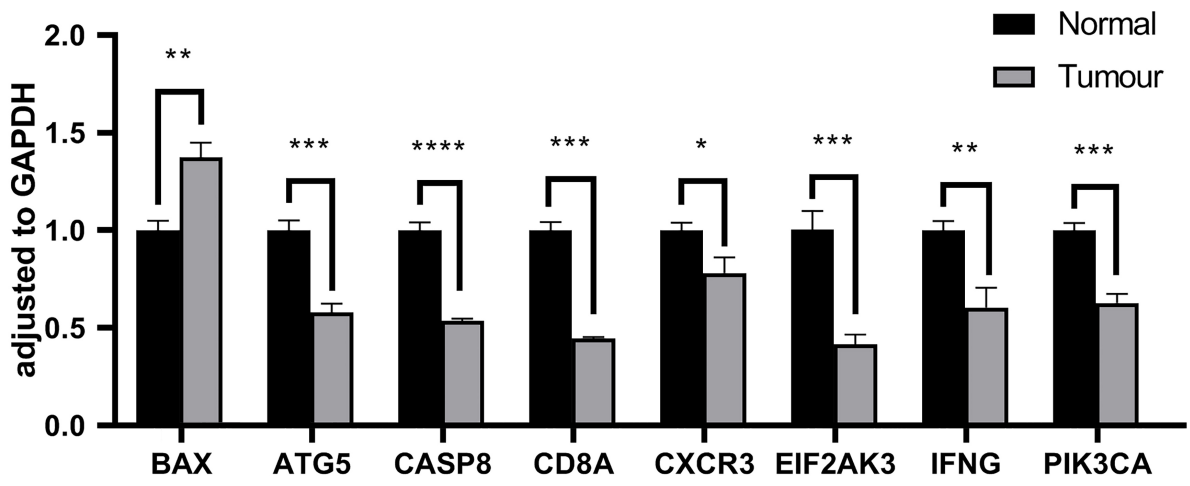

Fig. 9. Detection of expression levels of key ICD-related prognostic genes by qRT-PCR. The expression levels of 7 key genes in normal skin cells (black bar) and melanoma cells (grey bar) were determined by qRT-PCR. The statistical significance of expressional difference was visualized by * in figure (p-value < 0.0001: ****, p-value < 0.001: ***, p-value < 0.01: **, p-value < 0.05: *). qRT-PCR, quantitative reverse transcription polymerase chain reaction.

Journal of
BIOLOGICAL REGULATORS
and Homeostatic Agents

Validation of the Expressions of Key ICD-related Prognostic Genes by qRT-PCR

Contrasted to normal skin cells, melanoma cells exhibited a substantial increase in the expression of *BAX*, whereas the expressions of *ATG5*, *CASP8*, *CD8A*, *CXCR3*, *EIF2AK3*, *IFNG*, and *PIK3CA* were markedly decreased (Fig. 9).

Discussion

Early detection and targeted treatments have significantly improved the 5-year survival rate of melanoma patients, but the prognosis still remains poor [17]. Furthermore, the utilization of genetic characterization for prognosis remains limited despite significant innovations in understanding the genetic mechanisms of melanoma [18]. These deficiencies limit the treatment options for melanoma. Consequently, it is significant to explore new therapeutic targets and valid prognostic biomarkers for melanoma.

This study has identified two clusters by analyzing 33 ICD-related DEGs that are differentially expressed and related to ICD. These clusters presented distinct survival outcomes, with Cluster 1 displaying a notably elevated overall survival rate compared to Cluster 2. This provides clues for further research on melanoma.

After conducting functional enrichment analysis on the DEGs, the findings suggest that they have the potential to modulate signal recognition of the immune response, thereby boosting the immune system, particularly in terms of enhancing antibody-mediated immunity. The human immune system is responsible for distinguishing self-components and non-self-components to protect the organism from exogenous and endogenous antigens [19]. The immune system actively monitors tumor cells as potential targets, specifically identifying and mounting an attack against those that exhibit substantial antigenicity [20].

However, endogenous tumor-reactive immune cells are generally hyporesponsive or unresponsive to tumor cells in their natural status, mainly because tumor cells hide their antigens and develop immune tolerance [21]. Thus, during the process of ICD, antigens are submitted on the surface or secreted out of the tumor cells, activating endogenous tumor-reactive immune cells that recognize and lyse the tumor cells. This aligns with previous studies on ICD.

Subsequently, GSEA was performed. It was exhibited that the enriched GO pathways in Cluster 1 were tightly associated with the immune response against antigens, which is congruent with the better prediction of Cluster 1 in our study, as the human immune system can destroy tumor cells. GSEA analysis in Cluster 2 manifested that the characterized GO pathways were largely enriched in epidermal development, keratinization, skin water loss regulation, skin development, and keratinized envelope.

It was revealed that keratinocytes could secrete a melanocyte-stimulating hormone (MSH) which will bind to the melanocortin receptor 1 (MC1R) on melanocytes. This biological process induces their proliferation and promotes the release of melanin [22], forming the basis of melanoma generation. It is evident that active metabolic pathways in Cluster 2 are mainly correlated with melanoma development and progression, explaining the lower survival probability compared to Cluster 1. This provides research clues to the molecular mechanisms of melanoma development and progression.

As shown above, DEGs significantly correlate with the immune response to melanoma, and ICD significantly enhances anti-tumor immunity and melanoma eradication.

In comparison to Cluster 2, Cluster 1 exhibited an elevated immune score, matrix score, and ESTIMATE score, suggesting that patients with elevated expression of ICD-related genes may receive better outcomes from immunotherapy [23], consistent with previous consensus on melanoma treatment. Additionally, Cluster 1 displayed lower tumor purity, further supporting the notion of improved OS in these patients. It is proposed that these immune cells make a difference in the mechanism of ICD, making them potential targets for immunotherapies.

Previous studies have demonstrated that macrophage migration inhibitory factor (MIF) can facilitate the M2 polarization of macrophages associated with tumors and provide protection to tumor cells against ICD [24,25]. These findings suggest a potential detrimental impact of M2 macrophages on ICD, indicating that M2 macrophages may serve as an unfavorable prognostic indicator.

CD8+ T cells attack tumor cells, prompting the cells to release antigens, and may result in ICD [23,24]. Therefore, our findings are in line with the outcomes suggesting that patients with a high expression of ICD-related genes may exhibit an increased level of CD8+ T cells, which can have a positive impact on their prognosis.

Induced by DAMPs, dendritic cells (DCs) present antigens on the surface of dying cells. DCs encounter and turn naive CD4+ T cells into activated cells, including CD4+ memory-activated T cells [25–27]. It indicates that CD4+ memory-activated T cells are noteworthy to ICD and represent a good prognosis, consistent with our research.

The regulatory T cells (Tregs) are proven to antagonize ICD directly by expressing high levels of CD39 and CD73, two enzymes that can degrade ATP and prevent it from triggering ICD [28,29]. However, it is different from our results. The reason for the discrepancy will be elucidated by further research.

Cluster 1 demonstrated higher expression levels of all HLAs compared to Cluster 2. It has been found that HLA tightly corresponds with the prognosis and response to immunotherapy, with higher HLAs associated with longer survival in melanoma [30], which is consistent with our results. This finding has positive implications for research related to new therapeutic targets and effective prognostic biomarkers for melanoma. Thus, it was reconfirmed that increased

ICD-related gene expression is connected with better prognosis and therapeutic effects of immunotherapy.

The expression of *LAG3*, *SIGLEC15*, *CTLA4*, *HAVCR2*, *PDCD1LG2*, *PDCD1*, *TIGIT*, and *CD274* was remarkably higher in Cluster 1, suggesting that these genes could be explored as new targets for immunotherapy. It indicates that patients with higher expression of ICD-related genes tend to benefit from immunotherapy. T cells often co-express LAG3 and PD-1, and the simultaneous use of anti-LAG3 and anti-PD-1 antibodies produces a synergistic effect [4]. The phase 3 study, RELATIVITY-047, has demonstrated a correlation between the concurrent administration of anti-LAG3 and anti-PD-1 antibodies and enhancements in progression-free survival, compared to the use of anti-PD-1 antibodies alone. SIGLEC15 mediated inflammatory responses in tumor growth and was confirmed to be an attractive cell surface target for cancer immunotherapy [31]. The introduction of CTLA4 checkpoint inhibitors, including ipilimumab, nivolumab, and pembrolizumab, has significantly transformed the treatment of melanoma. Patients with advanced melanoma have greatly improved their OS with these inhibitors [32–36]. PDCD1, TIGIT, and CD274 checkpoints were also discovered to play a role in the development of cancer and may be promising targets for immunotherapy for melanoma in the future [37–39]. All of these studies strongly support our findings. The mentioned checkpoints hold great potential for clinical applications and have shown promise in enhancing the prognosis of melanoma, particularly when considering the genes connected to ICD that are highly expressed.

Our prognostic model, consisting of eight ICD-related DEGs, demonstrated significant effectiveness in prognostic evaluation. *BAX* is considered a risk gene, while the other seven DEGs (*ATG5*, *CASP8*, *CD8A*, *CXCR3*, *EIF2AK3*, *IFNG*, and *PIK3CA*) are considered protective genes. BAX, classified as a member of the BCL2 protein family, has the capability to bind with BCL2 protein, forming a heterodimer and serving as a stimulator of apoptosis. Patients with chemotherapy-treated metastatic melanoma with low levels of *BAX* experience improve progression-free survival (PFS) and can serve as a marker of improved PFS [40]. *CASP8* produces a caspase protein that belongs to a family of proteins responsible for triggering cell apoptosis through a series of sequential activations. The higher expression level of *CASP8* has been proven to have a more positive prognosis in cutaneous melanoma patients [41]. IFNG is a soluble cytokine belonging to the type II interferon family, inducing the expression of MHC-I and thus enhancing immunity. All eight DEGs have been shown to be involved in ICD through the same or different mechanisms. A prognostic model based on eight ICD-related DEGs shows remarkable consistency with survival rates, confirming its role in predicting the survival of melanoma patients.

The relevance analysis between specific immune cell abundance and risk scores revealed that distinct kinds of macrophages correlated differently with the risk scores depending on their differentiation direction. This information can contribute to providing more precise treatment for melanoma patients. The risk scores descend when the amount of M1 macrophages increases, while the results are the opposite when it comes to M0 and M2 macrophages. It has been demonstrated that M1 macrophages exhibit anti-cancer properties, whereas M2 tumor-associated macrophages (TAM) promote tumor growth [42]. Patients with primary melanoma were also verified to exhibit worse OS when more M0 macrophages were enriched in the tumor tissue [43]. These findings are consistent with our results, suggesting that the immune cell type and abundance have the potential to be indicators of personalized treatment for melanoma patients, providing strong support for the treatment of melanoma patients.

The present study acknowledges certain limitations. The sample size used was limited due to constraints, and the samples were not sourced from the GEO or TCGA databases, limiting their generalizability. Additionally, the non-standardized nature of the samples and variations in sample sizes across datasets may impact the accuracy of statistical analyses. To comprehensively evaluate the model's effectiveness and understand underlying mechanisms, further studies with a larger number of standardized samples are necessary. Furthermore, the assessment of ICD in this study is solely based on mRNA levels, and considering posttranscriptional modifications and protein regulation could provide a more nuanced understanding of ICD mechanisms [44]. Multi-omics studies would contribute to a deeper comprehension. Discrepancies in the impact of Tregs on ICD and the study's findings warrant further investigation, and future research should explore specific reasons for these differences.

Conclusions

In this study, we explored the immunological and prognostic functions of ICD-related DEGs in melanoma. The correlation between ICD and the immune infiltration landscape provides new insights for targeted therapy in melanoma. Additionally, we developed a risk-scoring model, leveraging eight DEGs associated with ICD, which demonstrated significant potential for prognostic prediction in melanoma. However, further research is necessary in the future to validate the role of ICD in melanoma.

Availability of Data and Materials

All data included in this study are available upon request by contact with the corresponding author. Available at drzhaojinmin@126.com.

Journal of
BIOLOGICAL REGULATORS
and Homeostatic Agents

Author Contributions

WL and LL designed the project. JZ contributed to administration and supervision of project. YL, BY, CP, RZ and LH collected data and performed analysis. RZ, YL and LH drafted the manuscript. JZ were responsible for provision of study materials or patients. All authors contributed to editorial changes in the manuscript. All authors read and approved the final manuscript. All authors have participated sufficiently in the work and agreed to be accountable for all aspects of the work.

Ethics Approval and Consent to Participate

Not applicable.

Acknowledgment

The authors thank the First Affiliated Hospital of Guangxi Medical University.

Funding

This research received no external funding.

Conflict of Interest

The authors declare no conflict of interest.

References

[1] Sanchez JA, Robinson WA. Malignant melanoma. Annual Review of Medicine. 1993; 44: 335–342.

[2] Bozkurt I, Yasar B, Baran Uslu M, Bozdogan N. A Primary Sacral Melanoma of Unknown Origin: A Case Report. Oncologie. 2022; 24: 163–171.

[3] Siegel RL, Miller KD, Jemal A. Cancer statistics, 2020. CA: a Cancer Journal for Clinicians. 2020; 70: 7–30.

[4] Ahmed B, Qadir MI, Ghafoor S. Malignant Melanoma: Skin Cancer-Diagnosis, Prevention, and Treatment. Critical Reviews in Eukaryotic Gene Expression. 2020; 30: 291–297.

[5] Parra LM, Webster RM. The malignant melanoma market. Nature Reviews. Drug Discovery. 2022; 21: 489–490.

[6] Kroemer G, Galluzzi L, Kepp O, Zitvogel L. Immunogenic cell death in cancer therapy. Annual Review of Immunology. 2013; 31: 51–72.

[7] Ahmed A, Tait SWG. Targeting immunogenic cell death in cancer. Molecular Oncology. 2020; 14: 2994–3006.

[8] Gao L, Gui R, Zheng X, Wang Y, Gong Y, Hua Wang T, *et al*. Topical Application of Houttuynia cordata Thunb Ethanol Extracts Increases Tumor Infiltrating CD8+ /Treg Cells Ratio and Inhibits Cutaneous Squamous Cell Carcinoma *in vivo*. Oncologie. 2022; 24: 565–577.

[9] Park SJ, Ye W, Xiao R, Silvin C, Padget M, Hodge JW, *et al*. Cisplatin and oxaliplatin induce similar immunogenic changes in preclinical models of head and neck cancer. Oral Oncology. 2019; 95: 127–135.

[10] Krysko DV, Garg AD, Kaczmarek A, Krysko O, Agostinis P, Vandenabeele P. Immunogenic cell death and DAMPs in cancer therapy. Nature Reviews. Cancer. 2012; 12: 860–875.

[11] Vandenabeele P, Vandecasteele K, Bachert C, Krysko O, Krysko DV. Immunogenic Apoptotic Cell Death and Anticancer Immunity. Advances in Experimental Medicine and Biology. 2016; 930: 133–149.

[12] Bommareddy PK, Zloza A, Rabkin SD, Kaufman HL. Oncolytic virus immunotherapy induces immunogenic cell death and overcomes STING deficiency in melanoma. Oncoimmunology. 2019; 8: 1591875.

[13] Wang X, Wu S, Liu F, Ke D, Wang X, Pan D, *et al*. An Immunogenic Cell Death-Related Classification Predicts Prognosis and Response to Immunotherapy in Head and Neck Squamous Cell Carcinoma. Frontiers in Immunology. 2021; 12: 781466.

[14] Xu M, Lu JH, Zhong YZ, Jiang J, Shen YZ, Su JY, *et al*. Immunogenic Cell Death-Relevant Damage-Associated Molecular Patterns and Sensing Receptors in Triple-Negative Breast Cancer Molecular Subtypes and Implications for Immunotherapy. Frontiers in Oncology. 2022; 12: 870914.

[15] Ruan H, Leibowitz BJ, Zhang L, Yu J. Immunogenic cell death in colon cancer prevention and therapy. Molecular Carcinogenesis. 2020; 59: 783–793.

[16] Garg AD, De Ruysscher D, Agostinis P. Immunological metagene signatures derived from immunogenic cancer cell death associate with improved survival of patients with lung, breast or ovarian malignancies: A large-scale meta-analysis. Oncoimmunology. 2015; 5: e1069938.

[17] Saginala K, Barsouk A, Aluru JS, Rawla P, Barsouk A. Epidemiology of Melanoma. Medical Sciences (Basel, Switzerland). 2021; 9: 63.

[18] Schadendorf D, van Akkooi ACJ, Berking C, Griewank KG, Gutzmer R, Hauschild A, *et al*. Melanoma. Lancet (London, England). 2018; 392: 971–984.

[19] Abbott M, Ustoyev Y. Cancer and the Immune System: The History and Background of Immunotherapy. Seminars in Oncology Nursing. 2019; 35: 150923.

[20] Kroemer G, Galassi C, Zitvogel L, Galluzzi L. Immunogenic cell stress and death. Nature Immunology. 2022; 23: 487–500.

[21] Pardoll D. Cancer and the Immune System: Basic Concepts and Targets for Intervention. Seminars in Oncology. 2015; 42: 523–538.

[22] Leonardi GC, Falzone L, Salemi R, Zanghì A, Spandidos DA, Mccubrey JA, *et al*. Cutaneous melanoma: From pathogenesis to therapy (Review). International Journal of Oncology. 2018; 52: 1071–1080.

[23] Minute L, Teijeira A, Sanchez-Paulete AR, Ochoa MC, Alvarez M, Otano I, *et al*. Cellular cytotoxicity is a form of immunogenic cell death. Journal for Immunotherapy of Cancer. 2020; 8: e000325.

[24] Jaime-Sanchez P, Uranga-Murillo I, Aguilo N, Khouili SC, Arias MA, Sancho D, *et al*. Cell death induced by cytotoxic $CD8^+$ T cells is immunogenic and primes caspase-3-dependent spread immunity against endogenous tumor antigens. Journal for Immunotherapy of Cancer. 2020; 8: e000528.

[25] Legrand AJ, Konstantinou M, Goode EF, Meier P. The Diversification of Cell Death and Immunity: Memento Mori. Molecular Cell. 2019; 76: 232–242.

[26] Yatim N, Cullen S, Albert ML. Dying cells actively regulate adaptive immune responses. Nature Reviews. Immunology. 2017; 17: 262–275.

[27] Xu MM, Pu Y, Han D, Shi Y, Cao X, Liang H, *et al*. Dendritic Cells but Not Macrophages Sense Tumor Mitochondrial DNA for Cross-priming through Signal Regulatory Protein α Signaling. Immunity. 2017; 47: 363–373.e5.

[28] Tanaka A, Sakaguchi S. Regulatory T cells in cancer immunotherapy. Cell Research. 2017; 27: 109–118.

[29] Vijayan D, Young A, Teng MWL, Smyth MJ. Targeting immunosuppressive adenosine in cancer. Nature Reviews. Cancer. 2017; 17: 765.

[30] Schaafsma E, Fugle CM, Wang X, Cheng C. Pan-cancer as-

sociation of HLA gene expression with cancer prognosis and immunotherapy efficacy. British Journal of Cancer. 2021; 125: 422–432.

[31] Wang J, Sun J, Liu LN, Flies DB, Nie X, Toki M, *et al*. Siglec-15 as an immune suppressor and potential target for normalization cancer immunotherapy. Nature Medicine. 2019; 25: 656–666.

[32] Robert C, Thomas L, Bondarenko I, O'Day S, Weber J, Garbe C, *et al*. Ipilimumab plus dacarbazine for previously untreated metastatic melanoma. The New England Journal of Medicine. 2011; 364: 2517–2526.

[33] Larkin J, Chiarion-Sileni V, Gonzalez R, Grob JJ, Rutkowski P, Lao CD, *et al*. Five-Year Survival with Combined Nivolumab and Ipilimumab in Advanced Melanoma. The New England Journal of Medicine. 2019; 381: 1535–1546.

[34] Robert C, Ribas A, Schachter J, Arance A, Grob JJ, Mortier L, *et al*. Pembrolizumab versus ipilimumab in advanced melanoma (KEYNOTE-006): post-hoc 5-year results from an open-label, multicentre, randomised, controlled, phase 3 study. The Lancet. Oncology. 2019; 20: 1239–1251.

[35] Larkin J, Chiarion-Sileni V, Gonzalez R, Grob JJ, Cowey CL, Lao CD, *et al*. Combined Nivolumab and Ipilimumab or Monotherapy in Untreated Melanoma. The New England Journal of Medicine. 2015; 373: 23–34.

[36] Robert C, Schachter J, Long GV, Arance A, Grob JJ, Mortier L, *et al*. Pembrolizumab versus Ipilimumab in Advanced Melanoma. The New England Journal of Medicine. 2015; 372: 2521–2532.

[37] Miao Y, Wang J, Li Q, Quan W, Wang Y, Li C, *et al*. Prognostic value and immunological role of PDCD1 gene in pan-cancer. International Immunopharmacology. 2020; 89: 107080.

[38] Chauvin JM, Zarour HM. TIGIT in cancer immunotherapy. Journal for Immunotherapy of Cancer. 2020; 8: e000957.

[39] Sun C, Mezzadra R, Schumacher TN. Regulation and Function of the PD-L1 Checkpoint. Immunity. 2018; 48: 434–452.

[40] Guttà C, Rahman A, Aura C, Dynoodt P, Charles EM, Hirschenhahn E, *et al*. Low expression of pro-apoptotic proteins Bax, Bak and Smac indicates prolonged progression-free survival in chemotherapy-treated metastatic melanoma. Cell Death & Disease. 2020; 11: 124.

[41] Mall R, Bynigeri RR, Karki R, Malireddi RKS, Sharma BR, Kanneganti TD. Pancancer transcriptomic profiling identifies key PANoptosis markers as therapeutic targets for oncology. NAR Cancer. 2022; 4: zcac033.

[42] Owen JL, Mohamadzadeh M. Macrophages and chemokines as mediators of angiogenesis. Frontiers in Physiology. 2013; 4: 159.

[43] Jairath NK, Farha MW, Jairath R, Harms PW, Tsoi LC, Tejasvi T. Prognostic value of intratumoral lymphocyte-to-monocyte ratio and M0 macrophage enrichment in tumor immune microenvironment of melanoma. Melanoma Management. 2020; 7: MMT51.

[44] Liu J, Chen Z, Zhao P, Li W. Prognostic and immune regulating roles of YIF1B in Pan-Cancer: a potential target for both survival and therapy response evaluation. Bioscience Reports. 2020; 40: BSR20201384.